

Quantifying Spatio-Temporal Variation of Invasion Spread

Joshua Goldstein¹, Murali Haran^{1*}, Ottar N. Bjørnstad² and Andrew Liebhold³

¹Department of Statistics, Pennsylvania State University, University Park, PA 16802 USA

*email: mharan@stat.psu.edu

²Departments of Entomology and Biology, Pennsylvania State University, University Park, PA 16802 USA

³US Forest Service Northern Research Station, Morgantown, WV 26505 USA

Abstract

The spread of invasive species can have far reaching environmental and ecological consequences. Understanding invasion spread patterns and the underlying process driving invasions are key to predicting and managing invasions. We develop a set of statistical methods to characterize local spread properties and demonstrate their application using historical data on the spread of the gypsy moth, *Lymantria dispar*, and hemlock wolly adelgid, *Adelges tsugae*. Our method uses a Gaussian process fit to the surface of waiting times to invasion in order to characterize the vector field of spread. Using this method we estimate with statistical uncertainties the speed and direction of spread at each location. Simulations from a stratified diffusion model verify the accuracy of our method. We show how we may link local rates of spread to environmental covariates for our two case studies.

Introduction

When a non-native species successfully establishes in an exotic environment it enters the spread phase of biological invasions during which it expands its range into suitable habitat (Lockwood et al., 2013). Ecological theory has shown that the speed of invasion spread is a joint function of the dispersal rate and the population growth rate of the invading species (Skellam, 1951; Okubo and Okubo, 1980); any habitat characteristic that influences population growth or dispersal can thus influence the rate of spread. Rates of spread may vary considerably among species and for a given species, spread rates may vary across heterogeneous landscapes (Shigesada et al., 1987; Tobin et al., 2007b). Understanding the mechanisms causing heterogeneity in the rate of invasion spread is key to predicting future rates of spread and to identifying important locations for management.

In this work we develop new methods for estimating local speed and dominant direction of spread along the invasion front. Our approach can be applied to identify statistically significant environmental and geographic determinants of local invasion rates.

In addition to environmentally-driven heterogeneity in rates of spread, there is considerable variation among species in the extent to which invasion spread is continuous. Spread of some species occurs via continuous expansion of the range into contiguous areas. For example, the North American muskrat, *Ondatra zibethica*, invaded central Europe from 1905-1927 via gradual expansion of its range in concentric circles (Skellam, 1951). The spread of other species is highly discontinuous, characterized by a pattern referred to as *stratified diffusion* (Shigesada et al., 1995); following initial establishment, expansion may happen with long-range jumps into isolated uninvaded areas, founding new colonies which expand

and eventually coalesce to form a contiguously invaded zone. This pattern is observed in many species of invading organisms, such as invasion of North America by the Argentine ant, *Linepithema humile* (Suarez et al., 2001) and the gypsy moth, *Lymantria dispar* (Sharov et al., 2002).

Quantifying the spread of non-native species and relating invasion speed to habitat heterogeneity is important for predicting and managing biological invasions. Several methods have been developed for measuring spread based upon fitting range size to time since establishment or estimating spread by directly quantifying displacement of range boundaries over time (Sharov et al., 1997; Tobin et al., 2007a; Gilbert and Liebhold, 2010). These methods are generally well-suited for quantifying average spread range and temporal variation therein, but they are limited in their ability to quantify local spread rates and their relation to local habitat characteristics. Also, these methods are generally designed to quantify spread as a continuous process; identification of long-range jumps in stratified dispersal is usually done visually in a non-automated fashion. These gaps in existing methodology provides our motivation for developing new and statistically rigorous methods for estimating local speed and direction of spread. We take advantage of recent statistical theory on the estimation of spatial gradients. We test our methods on simulated data generated from a stratified diffusion model and apply them to two detailed case studies of biological invasions, the historical spread of the gypsy moth and the hemlock wolly adelgid, *Adelges tsugae*, in North America.

Data

Gypsy moth

Native to Europe and Asia, the gypsy moth was accidentally introduced from France to Massachusetts in the late 1860's (Liebhold et al., 1989), it has since spread throughout much of the northeastern US. The gypsy moth is now established in a large area composed of the north Atlantic states and bordering Canadian provinces, as well as a second focus resulting from a long-range jump event to Michigan around 1980 (Liebhold et al., 1992; Johnson et al., 2006; Tobin et al., 2007b).

The invasion of the gypsy moth across North America has been rather slow compared to the rate of spread of many other alien species (Liebhold and Tobin, 2008). Mean spread was estimated at 21 km per year from 1960 to 1990 (Liebhold et al., 1992). The relatively slow rate of spread can be attributed, in part, to the fact that females of North America populations are flightless. Gypsy moth populations spread by short-range windborne dispersal of 1st instar larvae through a process known as 'ballooning' (Mason and McManus, 1981). Egg masses are also

accidentally transported on wood or human-made objects, forming new colonies ahead of the invasion front and resulting in a pattern of stratified diffusion (Sharov et al., 2002).

The full invasion history of the gypsy moth in the US is reflected in the year of government designation of gypsy moth quarantine by county. County-level quarantine records for gypsy moth are maintained by the United States Department of Agriculture (U.S. Code of Federal Regulations, Title 7, Chapter III, Section 301.45). Historically, an entire county was usually designated part of the quarantined area when established gypsy moth populations were first detected anywhere within the county. These records are updated annually and exist from 1934 to the present. From 1900 to 1934, the year when counties were first infested has been described in various other published sources (e.g., Burgess, 1913, 1915; Liebhold et al., 1992). As additional covariates, we used county-level data (Liebhold et al., 1997) on the percent of the forest basal area comprised of oaks, which is a favored food plant of the gypsy moth, and the size (km^2) of each county.

Hemlock wolly adelgid

Hemlock woolly adelgid (HWA) is an insect species responsible for mass defoliation of its host trees, eastern hemlock and Carolina hemlock (Orwig et al., 2002; Morin et al., 2009). Native to East Asia, it was first discovered in the USA in Virginia in the 1950s (Ward et al., 2004). HWA life stages can be transported by wind, wildlife, especially birds, and humans. Since its discovery, it has gradually expanded its range into much of the northeastern USA (Evans and Gregoire, 2007; Morin et al., 2009). By 1969 it was found in southern Pennsylvania and it invaded southern New England by 1985, spreading at an estimated speed of 20-30 km/year (Morin et al., 2009).

As with the gypsy moth, historical spread of the HWA was recorded at the county level. Records from the US Forest Service Forest Health Protection are available for 1951, 1971, 1981, 1996, and from 2001 to 2011. We use the basal area of hemlock (Morin et al., 2004) and plant hardiness zone (Cathey, 1990) for each county as additional covariates for our analysis.

Methods

Previous estimates of spread for gypsy moth data have estimated rates averaged over space. Liebhold et al. (1992) estimated spread rates for five geographic regions by the slope of a least-squares regression of time on distance to a reference point in each region. Spread rates have also been estimated by measuring the average

displacement of range boundaries over time (Sharov et al., 1997; Tobin et al., 2007a).

Previous research on estimating spatial gradients from georeferenced biological data has focused on detecting zones or boundaries of rapid change across space using geostatistical *wombling* (Womble, 1951). Wombling methods involve estimating local vector gradients by fitting bilinear functions over a lattice of points. This method has been applied to genetic (Barbujani et al., 1989) as well as ecological (Fortin, 1994) data. More recent wombling methods for areal data feature Bayesian hierarchical spatial models in order to identify significant boundaries after accounting for spatial dependence via Markov random fields (Banerjee et al., 2004; Fitzpatrick et al., 2010; Lu et al., 2007), with applications to ecology and epidemiology.

The use of spatial gradients to estimate biological spread is motivated by the fact that if the surface is the waiting time to first appearance, then the reciprocal of the gradient length is a measure of the invasion speed: Fast spread leads to shallow waiting time surfaces, while slow spread results in steep surfaces. Previously Johnson et al. (2004) estimated spread gradients using thin plate spline applied to waiting times (as measured by wavelet phase angles) to study outbreak dynamics of the larch budmoth. Farnsworth and Ward (2009) used a similar spline surface approach to study spread of avian influenza. The thin plate spline approach yielded gradients which reflect the magnitude and direction of the spread, a simple general-purpose approach for visualization, but has not associated errors with local spread estimates which prevents rigorous inference regarding whether, for example, any observed spatial variation is statistically significant.

Gaussian process gradient models

Banerjee et al. (2003) developed theory for estimating gradients of an arbitrary surface by specifying a Gaussian process model directly for the spatial gradients. We take advantage of this because when the gradients are defined on the waiting times to first appearance, the reciprocal of the gradient will represent the rate of spread.

We develop methods to rigorously test important features of the invasion, following existing theory (Banerjee et al., 2003; Banerjee and Gelfand, 2006). Below we further describe pattern recognition methods for detecting sites of long-range dispersals, radial expansion and directional patterns in historical spread. We also provide, in an electronic supplement, computer code for an R (Ihaka and Gentleman, 1996; R Core Team, 2013) software package that automates inference about spread.

We assume we have observations of the year of first appearance $\mathbf{Y} = \{Y(\mathbf{s}_1), \dots, Y(\mathbf{s}_n)\}$ at locations $\{\mathbf{s}_1, \dots, \mathbf{s}_n\}, \mathbf{s}_i \in \mathbb{R}^2$. For our examples, data are county-level quar-

tine records and the spatial locations $\{\mathbf{s}_1, \dots, \mathbf{s}_n\}$ are taken to be the centroids of counties for the gypsy moth where $n = 571$ counties (Figure 1a) and for the HWA where $n = 340$ counties (Figure 1b). Coordinates are projected using the Albers equal area conic projection with standard parallels $29^\circ 30'$ and $45^\circ 30'$. For county i , $Y(\mathbf{s}_i)$ is the year the county was added to the quarantine. We assume $Y(\mathbf{s})$ can be modelled using an isotropic Gaussian process with mean $\mu(\mathbf{s})$ and covariance $K(\cdot)$.

Banerjee et al. (2003) defines the finite difference directional derivative process at location \mathbf{s} for scale h in direction \mathbf{u} as

$$Y_{\mathbf{u},h}(\mathbf{s}) = \frac{Y(\mathbf{s} + h\mathbf{u}) - Y(\mathbf{s})}{h}$$

where \mathbf{u} is a unit vector. The directional derivative process in direction \mathbf{u} is then defined as

$$D_{\mathbf{u}}Y(\mathbf{s}) = \lim_{h \rightarrow 0} Y_{\mathbf{u},h}(\mathbf{s})$$

assuming the mean square limit exists. Of interest is the gradient of $Y(\mathbf{s})$ at \mathbf{s} , the vector of directional derivatives

$$\nabla Y(\mathbf{s}) = (D_{\mathbf{e}_1}Y(\mathbf{s}), D_{\mathbf{e}_2}Y(\mathbf{s}))$$

in orthonormal basis directions $\mathbf{e}_1 = (1, 0)$ and $\mathbf{e}_2 = (0, 1)$. Banerjee et al. (2003) shows there exists a joint trivariate Gaussian process for $Y(\mathbf{s})$ and $\nabla Y(\mathbf{s})$, and therefore \mathbf{Y} and $\nabla \mathbf{Y} = \{\nabla Y(\mathbf{s}_1), \dots, \nabla Y(\mathbf{s}_n)\}$ have a joint multivariate normal distribution which takes the form

$$\begin{pmatrix} \mathbf{Y} \\ \nabla \mathbf{Y} \end{pmatrix} \sim N_{3n} \left[\begin{pmatrix} \boldsymbol{\mu} \\ \nabla \boldsymbol{\mu} \end{pmatrix}, \begin{pmatrix} K(D) & -\nabla K(D) \\ \nabla K(D)^T & -H_K(D) \end{pmatrix} \right]$$

where D is the $n \times n$ matrix of pairwise Euclidean distances of \mathbf{s} , and $K(D)$ represents the $n \times n$ matrix of $K(\cdot)$ applied element-wise to D . $\nabla \boldsymbol{\mu}$ is the length $2n$ vector

$$\left(\frac{\partial \mu}{\partial x}(s_1), \dots, \frac{\partial \mu}{\partial x}(s_n), \frac{\partial \mu}{\partial y}(s_1), \dots, \frac{\partial \mu}{\partial y}(s_n) \right)^T,$$

$\nabla K(D)$ is the $n \times 2n$ matrix

$$\begin{pmatrix} \frac{\partial K}{\partial x}(D) & \frac{\partial K}{\partial y}(D) \end{pmatrix},$$

and $H_K(D)$ is the $2n \times 2n$ matrix

$$\begin{pmatrix} \frac{\partial^2 K}{\partial x^2}(D) & \frac{\partial^2 K}{\partial x \partial y}(D) \\ \frac{\partial^2 K}{\partial x \partial y}(D) & \frac{\partial^2 K}{\partial y^2}(D) \end{pmatrix}.$$

The conditional distribution of the gradient is therefore given by

$$\nabla \mathbf{Y} | \mathbf{Y}, \Theta \sim N_{2n} \left(\nabla \boldsymbol{\mu} - \nabla K(D)^T [K(D)]^{-1} (\mathbf{Y} - \boldsymbol{\mu}), -H_K(D) - \nabla K(D)^T [K(D)]^{-1} \nabla K(D) \right).$$

where Θ is a vector of mean and covariance parameters for the Gaussian process. Letting $\delta = (s_0 - s_1, \dots, s_0 - s_n)$, the estimated gradient at a point s_0 is given by

$$\begin{aligned} \nabla Y(s_0) | \mathbf{Y}, \Theta &\sim N_2 \left(\nabla \mu(s_0) - \nabla K(\delta)^T [K(D)]^{-1} (\mathbf{Y} - \boldsymbol{\mu}), \right. \\ &\quad \left. -H_K(0) - \nabla K(\delta)^T [K(D)]^{-1} \nabla K(\delta) \right). \end{aligned} \quad (1)$$

Note that for the gradient process to be well-defined, the original process must be mean square differentiable and all second order partial derivatives of K must exist. This is the case, for instance, when K is chosen to belong to the Matérn family with smoothness parameter $\nu > 1$ (Stein, 1999).

For our applications, we assume the original process $Y(\mathbf{s}) = \mu(\mathbf{s}) + w(\mathbf{s}) + \epsilon(\mathbf{s})$, with mean function $\mu(\mathbf{s}) = \beta_0 + \beta_1 s_x + \beta_2 s_y$, correlated spatial error $w(\mathbf{s}) \sim GP(0, K(\cdot))$ with Matérn covariance smoothness $\nu = 3/2$, which takes the explicit form $K(r) = \sigma^2(1 + \phi r) \exp\{-\phi r\}$, and uncorrelated error $\epsilon(\mathbf{s}) \sim N(0, \tau^2)$, where τ^2 is a nugget effect capturing both measurement error and microscale variability.

We infer the mean and covariance parameters $\Theta = (\beta_0, \beta_1, \beta_2, \sigma^2, \phi, \tau^2)$ based on a Bayesian approach using a Markov chain Monte Carlo (MCMC) algorithm. Flat prior distributions are assumed for mean parameters and inverse gamma priors are assumed for the partial sill (σ^2) and nugget (τ^2) with shape parameter 2 and scale parameter set to an approximate value from the empirical semivariogram. For the range (ϕ) a uniform prior is chosen with a support that allows the process to vary from low to high dependency. Simulation from the predictive distribution of the gradient can then be done by composition; given each posterior sample of Θ , a sample for $\nabla Y(s_0)$ can be drawn from (1).

At a given location s_0 , posterior samples are the gradient at s_0 in the x and y directions. When the data are times of first appearance, steeper gradients correspond to slower speeds. Therefore posterior estimates of the gradient (including Bayesian credible intervals) allow us to make inferences on the local speed and dominant direction of spread. Therefore the speed of spread is the inverse of the magnitude of the posterior gradient $\|\nabla Y(s_0)\|$, and the dominant direction of the spread is in the direction of the gradient $\nabla Y(s_0)/\|\nabla Y(s_0)\|$.

Detecting sources and long-range jumps

It is useful to have automated methods to identify candidate locations for foci of long-range jumps ahead of the advancing front as different from locations with contiguous “wave-like” diffusive spread. However, consistently identifying these foci is a challenge. We have identified two candidate solutions. The first borrows

methods from circular statistics, and the second is a more direct test of the average gradient orthogonal to a curve around the point.

The Rayleigh test (see e.g. Jammalamadaka and Sengupta, 2001) is a statistical test of whether a circular distribution is random or non-random. When applied to the vectors of spread near a point, a non-random distribution implies a unified directional spread through that point. We take directions of spread in a neighborhood around each centroid and test if these directions are drawn from a uniform circular distribution. Say we have n estimated directional vectors of spread x_i, y_i in a neighborhood around a point. Let r be the length of the mean vector from this sample, $r = \sqrt{\bar{x}^2 + \bar{y}^2}$. The test statistic is given by $R = 2nr^2$ for the test of

H_0 : Directional vectors are distributed randomly

H_a : Directional vectors are distributed non-randomly.

Under the null hypothesis R will be χ^2 distributed with 2 degrees of freedom. If the test fails to reject the null this may contribute evidence that the directional distribution is uniform as would be the case for radial spread from the point. While this may occur because the location is the point source of a long-range jump, the Rayleigh test will also flag areas with vectors that are converging to the point (akin to an ecological sink) or are truly random. Therefore while it is useful for flagging potential sites of long-range jumps, it is not a perfect method because we need to visually distinguish between the three different scenarios that all lead to failure to reject the null.

We also test directly the distribution of the gradient around a point, which will allow us to check if there is significant radial expansion around that point.

Define a curve $\mathcal{C}_{t^*} = \{s(t) : t \in [0, t^*]\}$, where $s(t) = (s_1(t), s_2(t)) \in \mathcal{R}^2$ and $s'(t)$ is the componentwise derivative. Let $\eta(s(t))$ be the unit vector normal to the curve at the point $s(t)$. The total gradient normal to \mathcal{C}_{t^*} is

$$\Gamma(t^*) = \int_0^{t^*} \langle \nabla Y(s(t)), \eta(s(t)) \rangle dv,$$

where v is the arc-length of the curve, $v(t^*) = \int_0^{t^*} \|s'(t)\| dt$, and so

$$\Gamma(t^*) = \int_0^{t^*} \langle \nabla Y(s(t)), \eta(s(t)) \rangle \|s'(t)\| dt,$$

In Banerjee and Gelfand (2006) it is shown that the distribution for the total gradient over a curve is a Gaussian process on $[0, T]$, $\Gamma(t^*) \sim GP(\mu_\Gamma(t^*), K_\Gamma(\cdot, \cdot))$ with

$$\mu_\Gamma(t^*) = \int_0^{t^*} \langle \mu(s(t)), \eta(s(t)) \rangle \|s'(t)\| dt$$

$$K_\Gamma(t_1^*, t_2^*) = \int_0^{t_1^*} \int_0^{t_2^*} \eta^T(s(t_1)) H_K [s(t_2) - s(t_1)] \eta(s(t_2)) \|s'(t_1)\| \|s'(t_2)\| dt_1 dt_2$$

where $\mu(\cdot)$ is the mean of the original process $Y(s)$ and $H_K(\cdot, \cdot)$ is the hessian of the covariance of $Y(s)$.

The conditional distribution of interest is

$$\Gamma(t^*) | \mathbf{Y}, \Theta \sim N(\mu_\Gamma - \gamma_\Gamma^T(t^*)[K(D)]^{-1}(\mathbf{Y} - \boldsymbol{\mu}), K_\Gamma(t^*, t^*) - \gamma_\Gamma^T(t^*)[K(D)]^{-1}\gamma_\Gamma(t^*))$$

where for $j = 1, \dots, n$

$$\gamma_\Gamma^T(t^*)_j = \text{cov}(\Gamma(t^*), Y(s_j)) = \int_0^{t^*} \langle K[s(t) - s(j)], \eta(s(t)) \rangle \|s'(t)\| dt.$$

The terms $\gamma_\Gamma(t^*)$ and $K_\Gamma(t^*, t^*)$ are not available analytically, and must be computed using numerical integration. The *average* gradient normal to the curve \mathcal{C}_{t^*} is simply the total gradient $\Gamma(t^*)$ divided by the arc-length.

Using this method centered on each location we can test the gradient normal to four sides of a box with sides of length r . As an heuristic we say if the spread is significantly *out* of at least two sides of the box, and does not go significantly *into* any side of the box, we will flag the location as a potential site of a long-range jump. We do this for a grid over the region of interest. In our figures, red lines indicate sides where there is a significant outward spread.

Driving factors of spread

We can gain insight into the mechanisms of spread by relating the geographic variation in spread to characteristics of habitat. To account for spatial dependence we fit a Bayesian spatial regression model to log-speeds of spread speed using the R package *spBayes* (Finley et al., 2007). We apply the log transformation to the response since the speeds have right-skewed distributions. If the mean speed at location \mathbf{s}_0 is given by $V(\mathbf{s}_0)$, then we assume

$$\log V(\mathbf{s}_0) = X^T(\mathbf{s}_0)\boldsymbol{\beta} + w(\mathbf{s}_0) + \epsilon(\mathbf{s}_0)$$

where $X(\mathbf{s})$ is a vector of the spatially varying environmental and geographical covariates of interest. $w(\mathbf{s}) \sim GP(0, G(\cdot))$, $G(\cdot)$ has Matérn covariance smoothness with smoothness ν , range ϕ and partial sill σ^2 and $\epsilon(\mathbf{s}) \sim N(0, \tau^2)$. Priors are selected as before and joint estimation is done via MCMC for $\{\boldsymbol{\beta}, \sigma^2, \phi, \tau^2, \nu\}$.

Results

Gypsy moth

Significant speeds and directions of historical spread of the gypsy moth are plotted at the locations of each county in the quarantine in Figure 2a. The mean speed

of spread over all counties is 20.8 km/year, with a median of 13.4 km/year. Distributions for the magnitude of spread at each location tend to be right skewed, where the average length of 95% credible intervals is 29.7 km/year.

In Figure 2b we test for sites of long-range dispersals using the two methods discussed above. For each method in practice we take circular neighborhoods of 1° . Points identified by the Rayleigh test are marked in black in Figure 2b, along with boxes where the gradient test is significant. Both methods identify three potential sites around the northeastern coast, Michigan and central-western Pennsylvania. Prior analysis confirms two of these sites, as the population was first introduced in Massachusetts in the 1860s and a discrete population was later established in Michigan (Liebhold et al., 1992). A close look at Figure 1a also highlights the jump to Centre County, PA in the mid 1970s.

We relate speed of spread to latitude and longitude, quarantine date, county size, and finally the percent basal area of trees preferred as hosts of the gypsy moth. Estimated parameters of the spatial regression model are given in Table 1a. We verify that on average the gypsy moth spread faster as it moved west. We also found that basal area of susceptible host trees is significantly associated with speed of spread, consistent with the concept that local growth rates will be larger in the face of more favorable habitat, and should consequently enhance invasion spread rates.

Hemlock woolly adelgid

Significant speeds and directions of spread for the HWA are plotted at each county in Figure 3a. We find a mean speed of spread of 20.5 km/year across counties, with a median speed of 13.5 km/year. The 95% credible intervals for spread at each location have an average length of 31.8 km/year.

Sites of long-range dispersal events are identified in Figure 3b. We detect areas of apparent long-range dispersals in Richmond and southern PA, suggesting a pattern of stratified diffusion. Morin et al. (2009) also found that expansion is significantly influenced by availability of host trees. Low winter temperatures can cause extensive mortality in HWA populations and limit expansion to the north (Trotter and Shields, 2009). Therefore we relate speeds of spread to environmental features including the presence or absence of hemlock trees, and the average plant hardiness zone for each county, an index based on the mean annual minimum winter temperature (Cathey, 1990). Estimates from the regression model are given in Table 1b. We observed evidence that historically expansion is faster to the west and north. We also find as in Morin et al. (2009) that spread is significantly associated with the abundance of host trees. We also tested the interaction between plant hardiness zone and latitude and found at a given latitude, HWA spread significantly slower through areas with lower plant hardiness zones

$[\beta = 3.4(0.4, 6.3)]$.

Simulation

We tested the ability of our method to recover the effects that spatially varying habitats have on the speed of spread. To accomplish this, data are simulated from a stratified diffusion model following Shigesada et al. (1995). Stratified diffusion is a combination of neighborhood diffusion and long distance dispersal. As the size of the original colony expands, new colonies are more likely to be created by long distance migrants.

The simulation starts with a single colony, centered at the initial point of invasion. The occupied area grows out in a circle, the radius r growing at constant rate c . This colony can then form offspring colonies from long-distance migrants in a random direction at a distance L from the invasion front. New colonies form at a rate $\lambda(r)$ that is a function of the colony radius. These offspring colonies grow at speed c and form offspring colonies of their own.

We begin with an initial introduction in Massachusetts in the year 1900. Colony range expansion c varies by longitude to simulate a slow period of initial expansion; $c = 10$ km/year east of -78° and $c = 20$ km/year west of -78° . New colonies form at rate $\lambda(r) = 0.1r$ a distance $L = 10$ km from the invasion front. Additionally, to mimic the observed Gypsy Moth data an artificial long-range jump is introduced in Michigan in 1950. The simulation is run for 107 years with an annual timestep.

The time until the invasion front reaches each county is recorded as the simulated quarantine data (Figure 4a). In Figure 4b we observe that our method of inference has successfully identified the two fixed colony introductions as regions of long-range jumps. We recover mean spread rates in the west of 10.7 km/year and in the east of 21.4 km/year, close to the actual values used in the simulation.

Discussion

To study the establishment and spread of biological invasions we present a new method to estimate local rates and direction of spread, and identify key spatial features including sources, sites of rapid spread and long-range jumps. We visualize and make inferences on historical patterns of spread of the gypsy moth and hemlock woolly adelgid as well as validate the methodology on simulated data. Posterior inference in a Bayesian setting allows us to test the significance of spread patterns and spatial features of these invasions in a rigorous way.

Taking our local estimates of gypsy moth spread and averaging them across time yields results in line with previous estimates in the literature (Liebhold et al., 1992). We find an average speed of 11.4 km/year across counties quarantined from

1900 to 1915, followed by a slow spread (5.0 km/year) across counties from 1916 to 1965 and then a period of very rapid expansion (25.8 km/year) from 1966 to 2000. These changes may also be related to the differences in Allee effects among different regions along the invasion front as evidenced in Tobin et al. (2009). From 2000 to present, coincident with the “Slow the Spread” program of control (Sharov et al., 2002) we observed an average speed of 14.6 km/year.

Our estimates for the spread of HWA when spatially averaged are also in line with estimates from the literature (e.g. Ward et al. (2004)). There is evidence that HWA range expansion is limited both by a lack of host trees and in the north by extreme winter temperatures. We also observe the spread of HWA to appear less diffusive than the gypsy moth. One explanation for this is the important role of wildlife, especially migratory birds, as a mechanism for HWA dispersal (McClure, 1990) in addition to windborne dispersal and human transport, which also accounts for anisotropy in spread observed in Morin et al. (2009).

Our abilities to identify patterns of spread are constrained by the spatial and temporal resolution of our data. County-level quarantine data are typically coarser than, for example, gypsy moth pheromone trap count data, though Tobin et al. (2007a) showed the two sources of gypsy moth data provided similar estimates. Additionally, the original Gaussian process must be sufficiently smooth for a gradient process to exist (we take the Matern model with smoothness parameter $\nu = 3/2$), with the consequence that some information is lost at small scales. We rely for the most part on annual records, but before 2001 the range of HWA was recorded at less frequent intervals. This is a potential source of bias in our early estimates of HWA spread.

For large spatial datasets, fitting a Gaussian process is a computational burden. Once the original Gaussian process is fit, however, we can draw samples by composition from the gradient process quickly. When the number of spatial locations is in the thousands we must likely have to rely on approximations such as the predictive process model of Banerjee et al. (2008).

Generally whenever the data are point-referenced waiting times, the speeds of spread can be estimated from the inferred gradient process. Therefore the methods presented here are generally applicable in ecology and epidemiology to spread of invasive species and infectious disease. These methods are also potentially applicable to non-invasion problems such as population waves such as the spread of an advantageous allele (Fisher, 1937), or recurrent outbreak waves in species such as the larch bud moth (Johnson et al., 2004). An R package that automates the inference is available as an electronic supplement.

Acknowledgements

This work has been funded by the Bill and Melinda Gates Foundation and by the National Science Foundation, #DEB-1354819.

Data Accessibility

We will put the data in the DRYAD data repository (www.datadryad.org).

References

Banerjee, S. and Gelfand, A. (2006). Bayesian wombling: Curvilinear gradient assessment under spatial process models. *Journal of the American Statistical Association*, 101(476):1487–1501.

Banerjee, S., Gelfand, A., and Sirmans, C. (2003). Directional rates of change under spatial process models. *Journal of the American Statistical Association*, 98(464):946–954.

Banerjee, S., Gelfand, A. E., and Carlin, B. P. (2004). *Hierarchical modeling and analysis for spatial data*. CRC Press.

Banerjee, S., Gelfand, A. E., Finley, A. O., and Sang, H. (2008). Gaussian predictive process models for large spatial data sets. *Journal of the Royal Statistical Society: Series B (Statistical Methodology)*, 70(4):825–848.

Barbujani, G., Oden, N., and Sokal, R. (1989). Detecting regions of abrupt change in maps of biological variables. *Systematic Biology*, 38(4):376–389.

Burgess, A. (1913). *The dispersion of the gypsy moth*. Number 119. United States Department of Agriculture.

Burgess, A. (1915). *Report on the gipsy moth work in New England*. Number 204. United States Department of Agriculture.

Cathey, H. M. (1990). USDA plant hardiness zone map. *U.S.D.A. Misc. Publ.*, (1475).

Chen, M.-H., Shao, Q.-M., and Ibrahim, J. G. (2000). *Monte Carlo methods in Bayesian computation*. Springer New York.

Evans, A. M. and Gregoire, T. G. (2007). A geographically variable model of hemlock woolly adelgid spread. *Biological Invasions*, 9(4):369–382.

Farnsworth, M. L. and Ward, M. P. (2009). Identifying spatio-temporal patterns of transboundary disease spread: examples using avian influenza H5N1 outbreaks. *Veterinary research*, 40(3):1–14.

Finley, A. O., Banerjee, S., and Carlin, B. P. (2007). spBayes: An R package for univariate and multivariate hierarchical point-referenced spatial models. *Journal of Statistical Software*, 19(4):1–24.

Fisher, R. A. (1937). The wave of advance of advantageous genes. *Annals of Eugenics*, 7(4):355–369.

Fitzpatrick, M. C., Preisser, E. L., Porter, A., Elkinton, J., Waller, L. A., Carlin, B. P., and Ellison, A. M. (2010). Ecological boundary detection using Bayesian areal wombling. *Ecology*, 91(12):3448–3455.

Fortin, M.-J. (1994). Edge detection algorithms for two-dimensional ecological data. *Ecology*, pages 956–965.

Gilbert, M. and Liebhold, A. (2010). Comparing methods for measuring the rate of spread of invading populations. *Ecography*, 33(5):809–817.

Ihaka, R. and Gentleman, R. (1996). R: A language for data analysis and graphics. *Journal of Computational and Graphical Statistics*, 5(3):299–314.

Jammalamadaka, S. R. and Sengupta, A. (2001). *Topics in circular statistics*, volume 5. World Scientific.

Johnson, D. M., Bjørnstad, O. N., and Liebhold, A. M. (2004). Landscape geometry and travelling waves in the larch budmoth. *Ecology Letters*, 7(10):967–974.

Johnson, D. M., Liebhold, A. M., Tobin, P. C., and Bjørnstad, O. N. (2006). Allee effects and pulsed invasion by the gypsy moth. *Nature*, 444(7117):361–363.

Liebhold, A., Mastro, V., and Schaefer, P. (1989). Learning from the legacy of Leopold Trouvelot. *Bulletin of the ESA*, 35(2):20–22.

Liebhold, A. M., Gottschalk, K. W., Luzader, E. R., Mason, D. A., Bush, R., and Twardus, D. B. (1997). Gypsy moth in the United States: An Atlas. *General Technical Report-Northern Research Station, USDA Forest Service*, (NE-233).

Liebhold, A. M., Halverson, J. A., and Elmes, G. A. (1992). Gypsy moth invasion in North America: A quantitative analysis. *Journal of Biogeography*, 19(5):513–520.

Liebhold, A. M. and Tobin, P. C. (2008). Population ecology of insect invasions and their management. *Annual Review of Entomology*, 53:387–408.

Lockwood, J. L., Hoopes, M. F., and Marchetti, M. P. (2013). *Invasion ecology*. John Wiley & Sons, New York.

Lu, H., Reilly, C., Banerjee, S., and Carlin, B. (2007). Bayesian areal wombling via adjacency modeling. *Environmental and Ecological Statistics*, 14(4):433–452.

Mason, C. and McManus, M. (1981). Larval dispersal of the gypsy moth. *The gypsy moth: research toward integrated pest management. US Department of Agriculture Technical Bulletin*, 1584:161–202.

McClure, M. S. (1990). Role of wind, birds, deer, and humans in the dispersal of hemlock woolly adelgid (Homoptera: Adelgidae). *Environmental Entomology*, 19(1):36–43.

Morin, R. S., Liebhold, A. M., and Gottschalk, K. W. (2009). Anisotropic spread of hemlock woolly adelgid in the eastern United States. *Biological Invasions*, 11(10):2341–2350.

Morin, R. S., Liebhold, A. M., Luzader, E. R., Lister, A. J., Gottschalk, K. W., and Twardus, D. B. (2004). Mapping host-species abundance of three major exotic forest pests. *USDA Forest Service Northeastern Research Station Research Paper*, (NE-726).

Okubo, A. and Okubo, A. (1980). *Diffusion and ecological problems: mathematical models*, volume 10. Springer-Verlag Berlin.

Orwig, D. A., Foster, D. R., and Mausel, D. L. (2002). Landscape patterns of hemlock decline in New England due to the introduced hemlock woolly adelgid. *Journal of Biogeography*, 29(10-11):1475–1487.

R Core Team (2013). *R: A Language and Environment for Statistical Computing*. R Foundation for Statistical Computing, Vienna, Austria.

Sharov, A. A., Leonard, D., Liebhold, A. M., Roberts, E. A., and Dickerson, W. (2002). “Slow The Spread”: A national program to contain the gypsy moth. *Journal of Forestry*, 100(5):30–36.

Sharov, A. A., Liebhold, A. M., and Roberts, A. E. (1997). Methods for monitoring the spread of gypsy moth (Lepidoptera: Lymantriidae) populations in the Appalachian Mountains. *Journal of Economic Entomology*, 90(5):1259–1266.

Shigesada, N., Kawasaki, K., and Takeda, Y. (1995). Modeling stratified diffusion in biological invasions. *American Naturalist*, pages 229–251.

Shigesada, N., Kawasaki, K., and Teramoto, E. (1987). The speeds of traveling frontal waves in heterogeneous environments. In *Mathematical Topics in Population Biology, Morphogenesis and Neurosciences*, pages 88–97. Springer.

Skellam, J. G. (1951). Random dispersal in theoretical populations. *Biometrika*, 38(1/2):196–218.

Stein, M. L. (1999). *Interpolation of spatial data: some theory for kriging*. Springer Science & Business Media.

Suarez, A. V., Holway, D. A., and Case, T. J. (2001). Patterns of spread in biological invasions dominated by long-distance jump dispersal: insights from Argentine ants. *Proceedings of the National Academy of Sciences*, 98(3):1095–1100.

Tobin, P. C., Liebhold, A. M., and Anderson Roberts, E. (2007a). Comparison of methods for estimating the spread of a non-indigenous species. *Journal of Biogeography*, 34(2):305–312.

Tobin, P. C., Robinet, C., Johnson, D. M., Whitmire, S. L., Bjørnstad, O. N., and Liebhold, A. M. (2009). The role of Allee effects in gypsy moth, *Lymantria dispar* (L.), invasions. *Population Ecology*, 51(3):373–384.

Tobin, P. C., Whitmire, S. L., Johnson, D. M., Bjørnstad, O. N., and Liebhold, A. M. (2007b). Invasion speed is affected by geographical variation in the strength of Allee effects. *Ecology Letters*, 10(1):36–43.

Trotter, R. T. and Shields, K. S. (2009). Variation in winter survival of the invasive hemlock woolly adelgid (Hemiptera: Adelgidae) across the eastern United States. *Environmental Entomology*, 38(3):577–587.

Ward, J. S., Montgomery, M. E., Cheah, C. A.-J., Onken, B. P., and Cowles, R. S. (2004). Eastern hemlock forests: guidelines to minimize the impacts of hemlock woolly adelgid. *USDA Forest Service Northeastern Research Station Research Paper*.

Womble, W. H. (1951). Differential systematics. *Science*, 114(2961):315–322.

Table 1: Results of a spatial regression of speeds of spread (km/year) for the gypsy moth (a) and hemlock wolly adelgid (b) including posterior means and 95% credible intervals obtained using the highest posterior density interval algorithm (Chen et al., 2000).

(a) Gypsy Moth		β
Intercept		-1.6(-11.0, 9.3)
Longitude		-5.1(-8.1, -2.2)
Latitude		-2.3(-6.6, 1.2)
County size		-0.00007(-0.00020, 0.00002)
Quarantine date		0.0006(-0.0044, 0.0056)
Basal% susceptible trees		0.0023(0.0000, 0.0042)
(b) HWA		β
Intercept		19.5(3.1, 36.6)
Longitude		-9.8(-14.9, -4.8)
Latitude		8.5(1.7, 16.0)
Quarantine date		-0.003(-0.009, 0.003)
$I_{\text{presence of hemlock}}$		0.09(0.01, 0.07)
Plant hardiness zone		0.014(-0.19, 0.23)

Figure 1: Year of first appearance by county for the gypsy moth (a) and hemlock woolly adelgid (b).

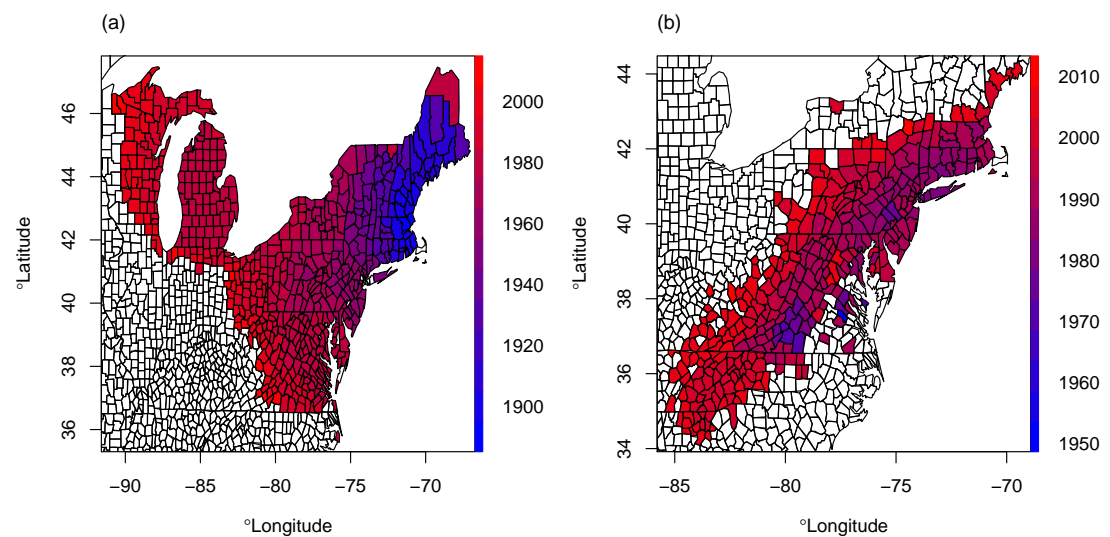


Figure 2: (a) Patterns of spread of the gypsy moth. Arrows indicate local speeds and directions of spread, and are plotted where spread is significant. (b) Identifying long-range jumps for the gypsy moth invasion. Black points are potential sites of long-range jumps identified by the Rayleigh test. Red boxes around a point indicate regions of potential long-range jumps identified by the grid search method (lines indicate sides of a box around a potential source where the spread was significantly out of the box).

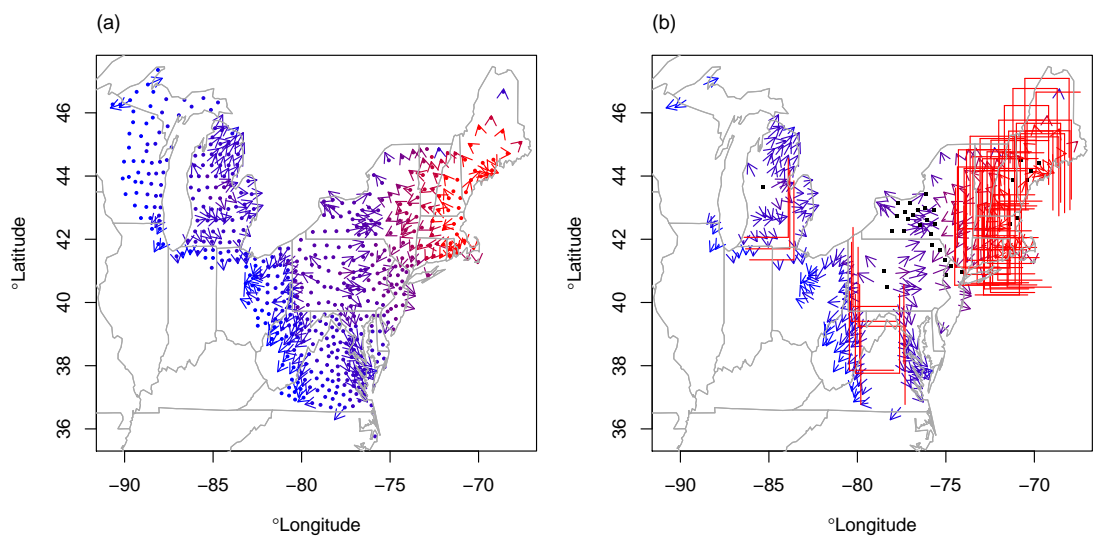


Figure 3: (a) Patterns of spread of the hemlock wolly adelgid. Arrows indicate local speeds and directions of spread, and are plotted where spread is significant. (b) Identifying long-range jumps for the gypsy moth invasion. Black points are potential sites of long-range jumps identified by the Rayleigh test. Red boxes around a point indicate regions of potential long-range jumps identified by the grid search method (lines indicate sides of a box around a potential source where the spread was significantly out of the box).

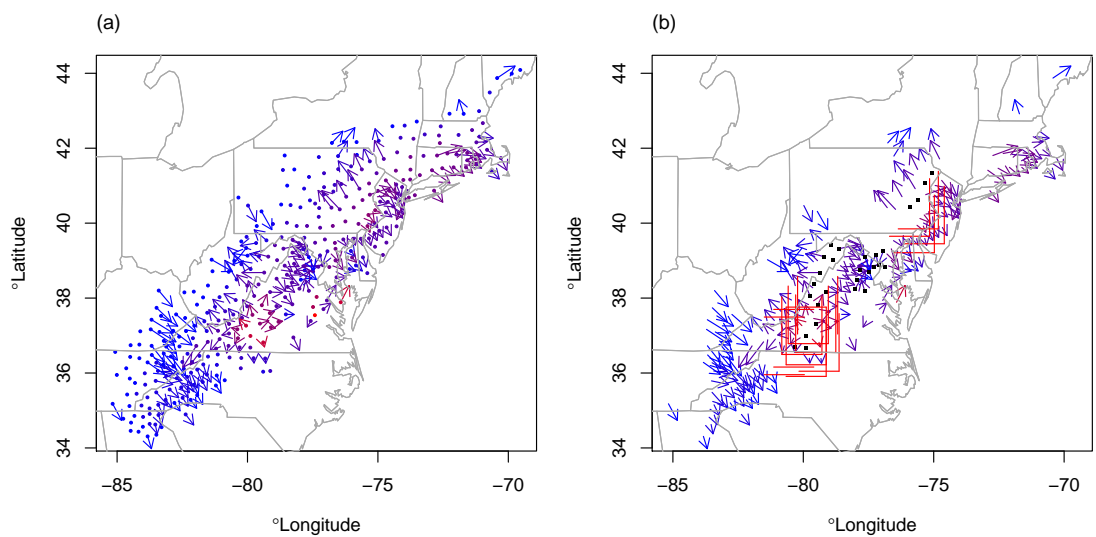


Figure 4: (a) Waiting times of the stratified diffusion simulation following Shigesada et al. (1995). (b) Long-range jumps for the simulated invasion. Black points are potential sites of long-range jumps identified by the Rayleigh test. Red boxes around a point indicate regions of potential long-range jumps identified by the grid search method.

